High density lipoprotein subpopulations from galactosamine-treated rats and their transformation by lecithin:cholesterol acyltransferase

Janet E. Matsuura and John B. Swaney

Department of Biological Chemistry, Hahnemann University, Philadelphia, PA 19102

Abstract It is known that an acute hepatotoxicity is produced in rats by intraperitoneal administration of galactosamine; a consequence of this treatment is a marked deficiency of lecithin:cholesterol acyltransferase (LCAT) activity in the plasma compartment. In this study high density lipoprotein (HDL) from galactosamine-treated rats was isolated, resolved into subpopulations, and characterized. In contrast to HDL from control rats, which elutes from gel filtration columns as a single peak and has a diameter of 13.1 nm, HDL from the galactosamine-treated animals was found to elute in five major zones with diameters of 7.8–35 nm. Characterization of these subpopulations has revealed that the larger fractions are enriched in apolipoprotein E, phospholipid, and cholesterol, but contain little cholesteryl ester, while the smallest two fractions contain mainly apolipoprotein A-I, are enriched in phospholipid, and have 50–60% of their cholesterol in the ester form. Incubation of HDL from treated rats with a source of LCAT activity plus low and very low density lipoproteins caused transformation of these subpopulations into a species which, by size and composition, was essentially identical to control rat HDL. In addition, when the subpopulations were individually incubated with purified human lecithin:cholesterol acyltransferase and bovine serum albumin, there was a similar convergence toward a moderate particle size approximating control rat HDL. Cross-linking studies showed that incubation with LCAT activity reduced the heterogeneity of the treated rat HDL. We conclude that the galactosamine treatment induces a complex mixture of HDL that bears strong similarities to the small, apoA-I rich and large, apoE-rich particles seen in LCAT deficiency or secreted by hepatic cells in culture. Furthermore, these species appear to coalesce in the presence of the $d > 1.21$ g/ml fraction of control serum to yield a fairly homogeneous population that resembles control rat HDL in size, composition, and apoprotein content. — **Matsuura, J. E., and J. B. Swaney**. High density lipoprotein subpopulations from galactosamine-treated rats and their transformation by lecithin:cholesterol acyltransferase. *J. Lipid Res.* 1991. **32:** 581–594.

Supplementary key words apolipoprotein • cross-linking • cholesterol • cholesteryl ester

Nascent HDL, the polar lipid-rich precursors to plasma HDL, are newly formed lipoproteins that exist only transiently in the plasma. Either newly secreted by liver or intestinal cells or generated as polar lipid-rich fragments of very low density lipoproteins (VLDL) or chylomicrons after triglyceride hydrolysis, these HDL are believed to be favored substrates in the lecithin:cholesterol acyltransferase (LCAT) reaction. These species undergo transformation to plasma HDL, primarily as a consequence of LCAT-mediated formation of hydrophobic cholesteryl esters (CE) from cholesterol and phosphatidylcholine (1–3).

The majority of nascent HDL is thought to possess a discoidal morphology due to a paucity of core lipids (e.g., triglyceride and cholesteryl ester); in generating CE, LCAT effects a disc-to-sphere transformation. Discoidal HDL have been isolated from a number of sources, including liver perfusates from rats and African green monkeys, media from a human hepatoma cell line (HepG2), mesenteric lymph from rats, and plasma from patients with familial LCAT deficiency or LCAT deficiencies secondary to liver disease (1, 3–7). With the exception of the HDL isolated from mesenteric lymph, all of these discoidal HDL were reported to be enriched in apolipoprotein E.

In addition to discoidal HDL, populations of small spherical nascent HDL have also been isolated from a variety of sources, including media from mouse hepatocytes and HepG2 cells, liver perfusates from African green monkeys, rat mesenteric lymph, and plasma from patients with familial LCAT deficiency or with obstructive jaundice (4, 7–10). These HDL contain predominantly apoA-I, have Stokes diameters of 7.5–8.0 nm and are enriched in phospholipid and free cholesterol. Incubation of

Abbreviations: apo, apolipoprotein; BSA, bovine serum albumin; CE, cholesteryl ester; Chol, cholesterol; FC, free cholesterol; cHDL, control HDL; galN, galactosamine; gHDL, HDL from galactosamine-treated rats; HDL, high density lipoproteins; LDL, low density lipoproteins; LCAT, lecithin:cholesterol acyltransferase; PL, phospholipid; DMPC, dimyristoylphosphatidylcholine; SDS-PAGE, sodium dodecyl sulfate polyacrylamide gel electrophoresis; TG, triglyceride; VLDL, very low density lipoproteins.

these HDL with a source of LCAT and free cholesterol was shown to generate larger spherical HDL (4, 11).

Sabesin, Kuiken, and Ragland (12) have shown that an experimental hepatotoxicity can be produced by injecting rats with galactosamine and that a major consequence of this treatment is a dramatic reduction in LCAT activity. Galactosamine induces an LCAT deficiency by trapping the liver's uridine pool as UDP-galactosamine derivatives and thereby inhibits UDP-dependent synthesis of glycoproteins, glycolipids, glycogen, nucleic acids, and a number of other macromolecules (13). Secretion of LCAT, which contains 24% carbohydrate by weight, is severely inhibited by galactosamine treatment. At 3 h post-galactosamine injection, LCAT activity levels fall to 25% of control values. By 24 h they are at 10% of control levels and the percentage of cholesterol as ester in serum is reduced five- to sixfold. HDL isolated from these animals are quite heterogeneous, but seem strikingly similar to HDL isolated from plasma of patients with familial LCAT deficiency in that they contain a range of particles, which include populations of large disks, large spheres, and small spheres (12, 14).

Although the galactosamine-induced hepatotoxicity could give rise to aberrant lipoprotein species, the HDL seen in this condition are of interest not only for understanding the effects of liver damage, but also because the low LCAT levels in these animals allow for study of lipoproteins that are prematurely halted in the maturation pathway. By isolating and characterizing individual HDL species, we undertook to establish the extent to which these HDL compare with other models of the LCAT-deficient state.

MATERIALS AND METHODS

Generation of galactosamine-treated serum pool

Male Sprague-Dawley rats (275–300 g) were obtained from Taconic Farms, Inc. (Germantown, NY) and were housed in the animal care facilities for at least a week before experimentation was begun; at the onset of the experiment the average weight of the animals was 300–350 g. The procedure of Cartwright et al. (14) was used with slight modification to produce an acute hepatotoxicity leading to an LCAT deficiency. Briefly, after an overnight fast, the animals were given an intraperitoneal injection of 1000 mg/kg of galactosamine (galN) prepared as a solution of 350 mg galN/ml 0.9% NaCl for experimental animals or an equal volume of the 0.9% NaCl solution for control animals.

The animals were fasted for an additional 24 h and then were exsanguinated from the abdominal aorta under methoxyflurane anesthesia. The blood was allowed to clot on ice and the serum was collected. Free and total cholesterol were measured by enzymatic assays and the percentage of cholesterol as ester was calculated for each serum sample. Sera with percentages of 25% CE or less were pooled to form the experimental group. Initially, only sera with percentages of 15% or less were pooled as had been suggested by Cartwright et al. (14), but it was found that the size and composition of the HDL isolated from sera that had percentages of esters of 15–25% were not significantly different from the HDL from sera with percentages of esters of 15% or less, so the experimental group was expanded to include sera with percentages up to 25%.

Isolation of HDL

Isolation of the galactosamine-treated rat HDL (gHDL) and the HDL from control fasted animals (cHDL) in the density range of d 1.07–1.23 g/ml was accomplished using isopycnic ultracentrifugation; for most experiments this required three centrifugation steps. Solid KBr was added to the sera pools to adjust the density to 1.07 g/ml and the samples were centrifuged in a Beckman 70 Ti rotor at 40,000 rpm for 16 h at 15°C. The density of the infranatant was adjusted to 1.23 g/ml with solid KBr and centrifugation was conducted at 35,000 rpm for 44 h. The d 1.07–1.23 g/ml fraction was recentrifuged at a density of 1.23 g/ml to remove albumin.

Separation of gHDL fractions by gel filtration

The gHDL was applied to a Bio-Gel A-1.5 m agarose column (1.6 × 90 cm) connected in series to a Bio-Gel A-0.5 m agarose column of the same dimensions (Bio-Rad, Richmond, CA). The columns were equilibrated with a 20 mM Tris-HCl, 0.15 M NaCl, 0.01% NaN_3, and 0.01% EDTA, pH 7.2, buffer. The absorbance of the column effluent was monitored at 280 nm and 4-ml fractions were collected. Peak fractions were then pooled and concentrated using Amicon Centripreps and Centricons (Amicon, Danvers, MA) and dialyzed against the NaCl-EDTA buffer described above to remove Tris, which is known to interfere with the Lowry protein assay (15).

Determination of particle size

Pore-limit electrophoresis was conducted on pre-cast 4–30% polyacrylamide gels in a Pharmacia gel electrophoresis apparatus (Pharmacia-LKB, Piscataway, NJ) at 7°C for 3000 volt-hours. The protein was then stained with Coomassie blue and the gels were scanned to determine the Stokes diameter of the major bands by comparison with the R_f values (based upon albumin migration) for protein standards of known Stokes diameter run on the same gel. The hydrated Stokes diameter values used were: 17.0 nm for thyroglobulin, 12.2 nm for apoferritin, 10.2 nm for catalase, 8.1 nm for lactate dehydrogenase, and 7.1 nm for bovine serum albumin (16). In some instances, the R_f for rat LDL (Stokes diameter, 30 nm (12)), was used to extend the calibration curve to larger sizes.

Apolipoprotein composition

SDS-PAGE was performed on slab gels with an acrylamide gradient from 3–27% for 16 h at 38 V; the gel was stained for protein with Coomassie blue, scanned, and the percentages of apolipoprotein A-I, E, and A-IV were determined from the areas under the peaks after correcting for differences in staining intensities of the apolipoproteins. The areas under the peaks were divided by the following correction factors, 0.44 for apoA-IV, 0.54 for apoE, and 1.0 for apoA-I (Swaney, J. B., F. Braithwaite, and H. A. Eder, unpublished observations).

Isoforms of the apolipoproteins were separated by isoelectric focusing using the method of Gidez, Swaney, and Murname (17). HDL samples were prepared in an equal volume of tetramethylurea and applied to 7.5% polyacrylamide tube gels containing 6.8 M urea and the ampholyte, Bio-lyte 4/6 (Bio-Rad), and then electrophoresed overnight.

Chemical cross-linking of gHDL

Chemical cross-linking of the proteins of each HDL was carried out using the bifunctional reagent, dimethylsuberimidate (18). The cross-linked samples then underwent SDS-PAGE and the protein mass was calculated by comparing distances of migration of the main cross-linked bands with those of cross-linked standards of known mass run on the same gel.

Compositional analysis

Protein was determined by the Markwell modification of the Lowry assay (19). Free and total cholesterol were measured by enzymatic assays and cholesteryl ester mass values were calculated by taking the difference between free and total cholesterol measures and multiplying by a correction factor of 1.7. Phospholipid was quantitated by the Wako enzymatic assay which measures choline after it is released by phospholipase D (Wako Pure Chemical Industries, Ltd., Osaka, Japan). Values for phospholipid were also determined by phosphorus assay (20), but as values were not significantly different between the two assays, the Wako assay was routinely used. Triglycerides were assayed by an enzymatic kit (Craig Bioproducts, Streamwood, IL). All assays were conducted in duplicate for a given experiment.

Incubation of HDL in reconstituted serum

The gHDL and cHDL were incubated for 24 h at 37°C with the d> 1.21 g/ml density fraction of control rat serum, which served as a source of LCAT activity as well as providing albumin for binding of lysolecithin; in some cases control d > 1.07 g/ml serum fraction was added as a source of additional cholesterol. The product HDL were reisolated in the density interval of d 1.07–1.21 g/ml by ultracentrifugation.

LCAT purification and activity assay

LCAT was purified from human hyperlipidemic plasma using a procedure based on the method of Matz and Jonas (21). The plasma was first centrifuged at 27,000 *g* for 1 h to remove chylomicrons and then ultracentrifuged at d 1.21 g/ml at 54,000 rpm, 10°C for 36 h in a Beckman 70 Ti rotor. The clear zone was collected by slicing the tubes to remove the d > 1.21 g/ml fraction and then pipetting the clear layer above the bottom yellow zone. After dialysis against 10 mM Tris-HCl, 50 mM NaCl, 5 mM EDTA, pH 7.6, this fraction was applied to an Affi-gel blue affinity column (Bio-Rad) connected in a series to a DEAE-Sepharose CL-6B column (Sigma, St. Louis, MO). Elution from the DEAE-Sepharose column was achieved with a 75–200 mM gradient of NaCl in the Tris buffer. Fractions were assayed for LCAT activity and two peaks with enzyme activity were pooled, dialyzed against 5 mM sodium phosphate, 140 mM NaCl, pH 6.9, overnight.

This pool was then applied to a Bio-Gel HTP hydroxyapatite column (Bio-Rad). Fractions were eluted with a 10–60 mM sodium phosphate gradient. The LCAT activity was found to be associated with the fractions comprising the first large peak, which were pooled and dialyzed against the 5 mM sodium phosphate buffer overnight, and then concentrated by applying this pool to a second smaller hydroxyapatite column and eluting with a minimal volume of 60 mM sodium phosphate, 140 mM NaCl, pH 6.9. A final dialysis step was performed against 10 mM Tris-HCl, 5 mM EDTA, pH 7.6, and an additional concentration step using Amicon centricons was conducted for dilute samples.

Protein was assayed by Bradford assay (22) using immunoglobulin as standard (Bio-Rad). LCAT activity, expressed as nmol cholesterol esterified/h per ml sample volume, was measured using the LCAT activity assay of Chen and Albers (23), modified as described below. An apoA-I/DMPC/[^{3}H]cholesterol liposome substrate (1:250:12.5 mol/mol) was prepared as previously described (24) and substituted for the apoA-I/egg yolk phosphatidylcholine/cholesterol liposome substrate of the same molar ratio. Other modifications were made in the incubation time, which was extended from 15 min to 1 h, and in the sample volume, which varied from 5 to 100 μl, depending upon the degree of purification and dilution of the sample. The sample volume of 15 μl was maintained for plasma samples.

Incubation of gHDL fractions with purified LCAT

The gHDL fractions were incubated with purified human LCAT (110 U/ml, the activity level measured in control serum) and bovine serum albumin (5 g/dl) for 24 h at 37°C and then reisolated with a single centrifugation at a density of 1.21 g/ml using the 50 Ti rotor with

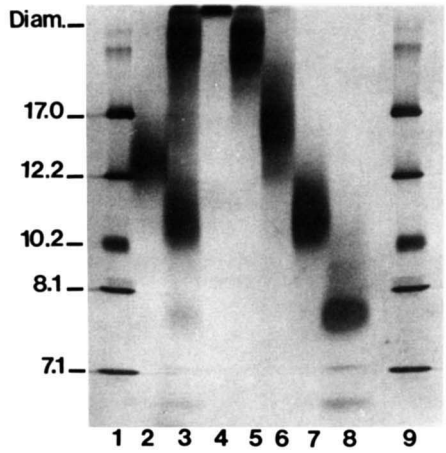

Fig. 1. Pore-limit electrophoresis of cHDL, gHDL, and gHDL column fractions. Lanes 1 and 9 contain protein standards (thyroglobulin, apoferritin, catalase, lactate dehydrogenase, and bovine serum albumin) and lane 2, cHDL; lane 3, gHDL; lane 4, $gHDL_{35+}$; lane 5, $gHDL_{30}$; lane 6, $gHDL_{16}$; lane 7, $gHDL_{11}$; and lane 8, $gHDL_{8}$. Lanes 2 and 5–8 contain 7.5 μg of HDL protein; lanes 3 and 4 contain 15 μg and 5 μg, respectively.

2-ml tubes. The HDL fractions were collected by tube slicing, dialyzed against 0.15 M NaCl, 2.7 mM EDTA, pH 7.6, and characterized.

RESULTS

Isolation of HDL

HDL were isolated as the d 1.07–1.23 g/ml density class, extending the normal density interval for rat HDL (d 1.07–1.21 g/ml) (25) to 1.23 g/ml to maximize the yield of the smallest, densest HDL isolated from galactosamine-treated rats. For control animals this density class contained minimal contamination from HDL_1 (d 1.05–1.07 g/ml) or low density lipoprotein (LDL), which had been seen as additional species eluting at or near the void volume when a density of 1.05–1.23 g/ml was used to isolate cHDL. For gHDL there was no discernible difference in the elution patterns when either a lower density cut of 1.05 g/ml or 1.07 g/ml was used. The protein concentration of the gHDL in serum was consistently found to be approximately one-third the value seen for cHDL (0.14 mg/ml serum for gHDL and 0.4 mg/ml for cHDL).

Particle Size

In order to evaluate the homogeneity of the HDL isolated from cHDL and gHDL, pore-limit electrophoresis on acrylamide gradient gels was performed; this showed very different patterns for cHDL and gHDL (**Fig. 1**, lanes 2 and 3). While cHDL yielded a single broad band with Stokes diameter of 13.1 ± 0.2 nm, gHDL was separated into a number of bands with Stokes diameters ranging from 7.8 to greater than 35.0 nm.

To isolate the individual gHDL species, the d 1.07–1.23 g/ml density class was applied to two gel filtration columns connected in series; the gHDL eluted as five major peaks which were separately pooled (**Fig. 2**). The names of the pools reflect their average Stokes diameter determined by pore-limit electrophoresis (Fig. 1, lanes 4–8). The largest species, $gHDL_{35+}$, which eluted with the void volume of the column, had a Stokes diameter of 34.5 ± 0.8 nm (lane 4). Despite the high absorbance value seen for this fraction, which is attributable to turbidity, this pool accounted for less than 10% of the protein recovered from the column. The second eluted fraction, $gHDL_{30}$ (Fig. 1, lane 5) was composed of two bands of Stokes diameters of 31.4 ± 0.9 nm and 27.8 ± 1.3 nm and represented approximately 30% of the protein recovered. As the $gHDL_{35+}$ and the $gHDL_{30}$ subfrac-

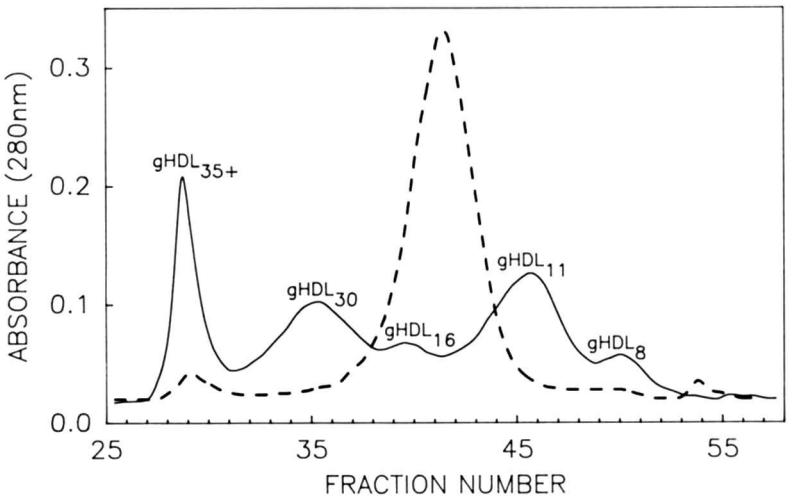

Fig. 2. Gel filtration of the d 1.07–1.23 g/ml fraction from control (-----) and galactosamine-treated rat sera (——) on a Bio-Gel A-1.5 m agarose column (1.6 × 90 cm) connected in series to a Bio-Gel A-0.5 m agarose column (1.6 × 90 cm). Fractions were pooled as follows: $gHDL_{35+}$ (27–29), $gHDL_{30}$ (32–36), $gHDL_{16}$ (38–40), $gHDL_{11}$ (43–46), and $gHDL_{8}$ (49–52).

tions were found to be at or above the largest standard used, their Stokes diameter assignments are considered to be tentative.

The next pool, $gHDL_{16}$, represented about 10% of the protein recovered and contained a number of bands; the two most prominent bands had Stokes diameters of 17.3 ± 0.6 nm and 15.4 ± 0.3 nm (Fig. 1, lane 6). The two remaining pools, $gHDL_{11}$ and $gHDL_8$, had Stokes diameters of 10.6 ± 0.3 nm and 7.8 ± 0.2 nm, respectively, and accounted for about 30% and 5% of the protein recovered. The remaining 15% of the recovered protein was associated with the fractions between the pooled fractions. In preliminary experiments the cHDL was also applied to the agarose column system. However, it was found that the cHDL eluted as a single broad peak, so in later experiments it was no longer applied to the columns.

Apolipoprotein composition

Studies of the cHDL, gHDL, and the gHDL gel filtration fractions by SDS-PAGE demonstrated that there was considerable variability in apolipoprotein composition of gHDL. In general, gHDL displayed a higher percentage of apoE and a lower percentage of apoA-IV than cHDL (**Fig. 3; Table 1**). Among the gHDL subfractions, the larger species, $gHDL_{35+}$ and $gHDL_{30}$ (Fig. 3, lanes 2 and 3), were enriched in apoE, while the smaller particles, $gHDL_{11}$ and $gHDL_8$, contained predominantly apoA-I (Fig. 3, lanes 5 and 6). The apolipoprotein composition of $gHDL_{16}$ was the most variable, possibly reflecting the greater number of subspecies making up this pool, but it was also the most similar to that of cHDL.

When applied to SDS-PAGE, the $gHDL_8$ subfraction was found to contain a band that migrated like apoA-IV

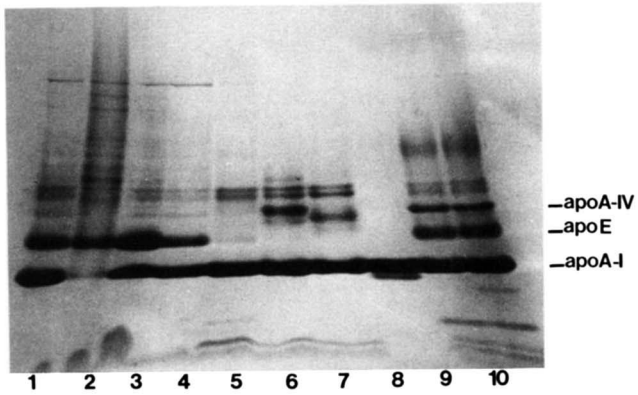

Fig. 3. SDS-PAGE of cHDL, gHDL, and gHDL column fractions. All samples were reduced with β-mercaptoethanol unless otherwise noted. Twenty μg of protein was applied to each lane. Lane 1, gHDL, lane 2, $gHDL_{35+}$, lane 3, $gHDL_{30}$, lane 4, $gHDL_{16}$, lane 5, $gHDL_{11}$, lane 6, $gHDL_8$, lane 7, $gHDL_8$ minus β-mercaptoethanol, lane 8, human apoA-I as a standard, lane 9, cHDL, and lane 10, cHDL minus β-mercaptoethanol.

TABLE 1. Apolipoprotein A-I, E, and A-IV composition in HDL subpopulations

HDL	ApoA-I	ApoE	ApoA-IV
		% of protein	
gHDL	50.5 ± 13.5	41.5 ± 15.5	7.9 ± 2.1
$gHDL_{35+}$ [a]	13.6 ± 6.7	80.2 ± 1.4	6.2 ± 5.4
$gHDL_{30}$	27.6 ± 5.1	65.7 ± 11.5	6.7 ± 7.7
$gHDL_{16}$	49.8 ± 14.1	39.9 ± 18.9	10.4 ± 4.9
$gHDL_{11}$	81.3 ± 4.8	6.5 ± 1.4	12.2 ± 5.6
$gHDL_8$	88.5 ± 3.0	0.0 ± 0.0	(11.5 ± 0.9)[b]
cHDL	49.3 ± 9.6	30.7 ± 11.9	20.0 ± 4.8

Mean of three experiments ± SD. The percentage of each apolipoprotein was derived from scans of 3–27% SDS-PAGE gels after correcting for differences in staining intensities by dividing by 0.44 for apoA-IV, 0.54 for apoE, and 1.0 for apoA-I.

[a] Mean of two experiments ± SD.

[b] This band migrates farther in the absence than in the presence of β-mercaptoethanol and is therefore not apoA-IV but an unknown protein. No correction in staining intensity was made for this unknown protein.

when the samples were reduced with β-mercaptoethanol (Fig. 3, lane 6). However, when β-mercaptoethanol was not added, this band migrated farther than apoA-IV (Fig. 3, lane 7). This type of an effect of β-metcaptoethanol on a protein is typical of that observed for reduction of intrachain disulfide bonds. Rat apoA-IV contains no disulfide bonds (26) and the migration of apoA-IV is not affected by β-mercaptoethanol treatment (Fig. 3, lane 9 vs. 10) (27). These data imply that this band is not apoA-IV. Alternative possibilities might include apoH, which has several internal disulfide bonds and a size compatible with these data, or α_1-acid glycoprotein, a protein of similar size that is known to become elevated with liver injury. That this protein is not apoA-IV appears to be supported by isoelectric focusing since, when the $gHDL_8$ subfraction was applied to an IEF gel with a pH range 4–6, only faint bands were visualized in the region where apoA-IV isoforms are usually seen (**Fig. 4**, lane 7); however, a cluster of bands was seen in the pH range of 4.8–5.3, a region that does not overlap with any of the pI values for the known rat apolipoproteins (17).

Dory et al. (28) have reported that newly synthesized apoE, secreted as a component of nascent HDL, are enriched in sialic acid residues as compared to apoE isolated from plasma lipoproteins, which band predominantly as isoforms containing no sialic acid residues. They proposed that apoE contained on nascent HDL is progressively desialylated during its lifetime in the plasma compartment. To ascertain whether the different species of gHDL might reflect different degrees of desialylation of apoE, isoelectric focusing was performed. Isoelectric focusing patterns of cHDL and gHDL (Fig. 4, lanes 1 and 2) did not demonstrate an altered proportion of the more acidic isoforms of apoE in gHDL when compared to cHDL (17). However, it is known that galactosamine

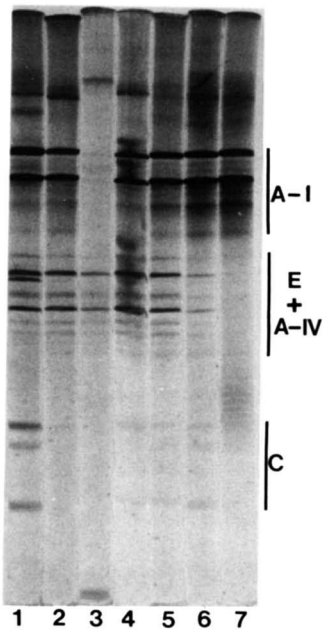

Fig. 4. Isoelectric focusing of cHDL, gHDL, and gHDL column fractions. Fifty μg aliquots were applied to 7.5% polyacrylamide tube gels containing 6.8 M urea and Bio-lyte 4/6 (ampholyte for the pH range 4–6) and electrophoresed overnight. Lane 1, cHDL, lane 2, gHDL, lane 3, $gHDL_{35+}$, lane 4, $gHDL_{30}$, lane 5, $gHDL_{16}$, lane 6, $gHDL_{11}$, lane 7, $gHDL_{8}$.

depletes the liver's uridine pool and can therefore severely inhibit glycosylation.

The IEF pattern for cHDL, though, did show some differences from that of gHDL. The cHDL contained a band at the more basic end of the apoE/apoA-IV isoform region, which was absent from gHDL and it also contained more protein in the apoC region than gHDL. The isoelectric focusing patterns seen for the individual gHDL subfractions were in agreement with the percentage of apoA-I, apoE, and apoA-IV determined from SDS-PAGE analysis (Table 1); for example, $gHDL_{35+}$ was relatively poor in apoA-I (Fig. 4, lane 3), while $gHDL_{11}$ and $gHDL_{8}$ were apoE poor (Fig. 4, lanes 6 and 7).

Chemical cross-linking

In an effort to quantitate the mass of protein that resides on each species of particles, chemical cross-linking of HDL followed by SDS-PAGE was performed (**Fig. 5**). The cHDL cross-links as a broad band with a protein mass of 153,000 ± 13,000 (lane 9). By contrast, cross-linking of the gHDL yields a number of bands, including bands corresponding to apoE monomer and dimer (lane 2). Cross-linking of the apoA-I-rich species, $gHDL_{11}$ and $gHDL_{8}$, yielded more homogeneous profiles: the predominant band for $gHDL_{11}$ was at 85,000 ± 3,000, while that for $gHDL_{8}$ was at 55,700 ± 2,100; these molecular weights correspond to those expected for A-I trimers and dimers, respectively.

The apoE-rich gHDL particles yielded much less homogenous cross-linked products than the apoA-I-rich gHDL. No discernible cross-linked mass was seen for $gHDL_{35+}$ (lane 3). $gHDL_{30}$ contained bands with an M_r corresponding to apoE monomer, dimer and trimer, and a faint broad band at 160,000 which may represent a maximum protein mass per particle. The $gHDL_{16}$ subfraction revealed a band with a mass of 140,000 ± 2,000, but still contained distinct apoE monomer and dimer bands.

Table 2 presents the particle mass, calculated by dividing the protein mass per particle as revealed by cross-linking by the protein weight percentage for a given HDL. The particle mass of the gHDL subfractions covered a range from 100,000 to over 600,000, composed of HDL particles both smaller and larger than cHDL.

Chemical Composition

The chemical composition of gHDL differs greatly from that of cHDL (**Table 3**). The gHDL are enriched in free cholesterol (16.7 ± 1.8% vs. 4.1 ± 0.8%) and phospholipid (51.4% ± 3.9% vs. 24.0 ± 1.5%), but contain much less protein (25.4 ± 4.3% vs. 37.8 ± 2.2%) and cholesteryl ester (6.6 ± 2.1% vs. 34.1 ± 3.3%) than cHDL. Additionally the percentage cholesterol esterification for gHDL (19.0 ± 5.3%) is much less than that for cHDL (83.0 ± 3.3%).

The apoE-rich species ($gHDL_{35+}$, $gHDL_{30}$, and $gHDL_{16}$) are enriched in FC and PL, but have much lower percentages of protein and CE as compared to cHDL. Like the apoE-rich gHDL, the apoA-I rich species, $gHDL_{11}$ and $gHDL_{8}$, are also enriched in PL. However, they are not enriched in FC and have a higher percentage of CE than apoE-rich HDL. Their level of percent esterification (50–60% cholesterol as ester), while lower than that for cHDL, is still significantly higher than that seen for the apoE-rich gHDL (4–20% cholesterol as ester) and indicates that these HDL have some cholesteryl ester core.

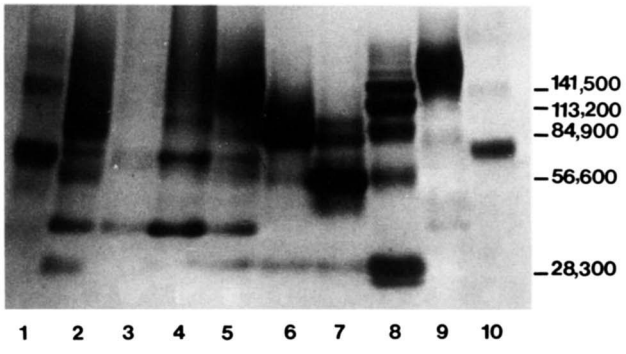

Fig. 5. SDS-PAGE of HDL species cross-linked with dimethylsuberimidate. Cross-linked BSA (lane 1), human apoA-I (lane 8), and hemocyanin (lane 10) were applied to the gel as standards. Twenty μg aliquots were applied to each lane: lane 2, gHDL, lane 3, $gHDL_{35+}$, lane 4, $gHDL_{30}$, lane 5, $gHDL_{16}$, lane 6, $gHDL_{11}$, lane 7, $gHDL_{8}$, and lane 9, cHDL.

TABLE 2. Particle mass of HDL subfractions

HDL	Cross-Linked Protein Mass ($\times 10^{-3}$)	Particle Mass ($\times 10^{-3}$)
$gHDL_{16}$	140.0 ± 2.0	610 ± 20
$gHDL_{11}$	85.0 ± 3.0	253 ± 10
$gHDL_{8}$	55.7 ± 2.1	106 ± 12
cHDL	152.7 ± 12.5	410 ± 37

Protein mass was determined by cross-linking with dimethylsuberimidate and particle mass was determined by dividing the protein mass by the protein weight percentage. Values are the mean of three experiments ± SD.

Incubation of HDL with d > 1.21 g/ml from serum

LCAT deficiency is a major characteristic of galactosamine treatment and we found that serum LCAT levels 24 h after galactosamine administration were less than 10% of serum levels of control fasted rats (10 nmol cholesterol esterified/h per ml vs. 110 nmol cholesterol esterified/h per ml). Therefore, it was of interest to learn whether LCAT activity from control serum is capable of converting the gHDL species to resemble cHDL. HDL incubated for 24 h at 37°C with the d > 1.21 g/ml density fraction from control rat serum with or without the d < 1.07 g/ml from control rat serum were reisolated by density ultracentrifugation and subjected to pore-limit electrophoresis (**Fig. 6**). Densitometric scans of this gel indicated that the Stokes diameter of cHDL increased from 12 to 14 nm when it was incubated with d > 1.21 g/ml, in agreement with previous observations (29). When the d < 1.07 g/ml fraction from control rat plasma was also included in the incubation mixture, the Stokes diameter of cHDL was increased further to 15 nm.

When gHDL was incubated with control rat d > 1.21 g/ml fraction, the complex banding pattern characteristic of gHDL was replaced with a more homogeneous profile; a major band with a Stokes diameter of 12 nm and a prominent shoulder at 15 nm were visible. Inclusion of the d < 1.07 g/ml fraction in the incubation mixture increased the Stokes diameter of the major band to 13 nm and a slightly narrower peak was formed.

To ascertain whether these changes were also manifested in altered protein stoichiometry, cross-linking studies were performed. The cross-linked mass for cHDL was increased when cHDL was incubated with d > 1.21 g/ml (**Fig. 7A**), but no additional increase was seen when the d < 1.07 g/ml fraction was included. The cross-linking pattern for gHDL changed dramatically when it was incubated with d > 1.21 g/ml (Fig. 7B). Before incubation the cross-linked pattern for gHDL included an apoA-I trimer and apoE monomer and dimer as well as numerous other minor bands, but after incubation a cross-linked species slightly larger than an apoA-I tetramer was formed and the apoE bands were diminished. Inclusion of the d < 1.07 g/ml fraction to the incubation mixture resulted in an increase in the cross-linked protein mass to slightly larger than an apoA-I pentamer and further loss of apoE bands occurred.

Chemical composition data for the products of HDL incubated with d > 1.21 g/ml and subsequently reisolated are shown in **Table 4**. Incubation of cHDL with d > 1.21 g/ml alone increased the percentage esterification from 79.2 to 96.9% and resulted in a gain in CE at the expense of FC and PL. A similar pattern was seen when the d < 1.07 g/ml fraction was included in the incubation, although the level of esterification was slightly less, probably as a result of the contribution of the VLDL and LDL to the free cholesterol pool.

Incubation of gHDL with control d > 1.21 g/ml fraction increased the percentage esterification threefold from 21.6 to 63.5%. This was accompanied by a loss in FC and PL and a gain in CE and in protein. Inclusion of the d < 1.07 g/ml fraction yielded a further increase in percentage cholesterol esterification and further losses in FC and PL. The chemical composition of the gHDL + d > 1.21 g/ml + d < 1.07 g/ml was essentially identical to that of the unincubated cHDL.

TABLE 3. Composition of HDL species

HDL	Weight % Composition				
	Protein	Phospholipid	Free Cholesterol	Cholesteryl Ester	% Cholesterol as Ester
gHDL	25.4 ± 4.3	51.4 ± 3.9	16.7 ± 1.8	6.6 ± 2.1	19.0 ± 5.3
$gHDL_{35+}$	21.5 ± 3.3	50.4 ± 7.3	25.0 ± 3.1	3.1 ± 1.6	6.6 ± 2.7
$gHDL_{30}$	14.0 ± 1.9	59.2 ± 3.4	23.1 ± 1.8	3.7 ± 2.0	8.5 ± 4.0
$gHDL_{16}$	22.6 ± 1.5	54.7 ± 2.1	17.7 ± 1.2	5.0 ± 1.8	14.3 ± 4.7
$gHDL_{11}$	32.6 ± 2.8	44.1 ± 2.6	6.0 ± 0.9	17.5 ± 1.7	63.8 ± 5.5
$gHDL_{8}$	50.7 ± 5.6	39.0 ± 5.3	3.5 ± 0.4	6.9 ± 0.8	53.7 ± 5.7
cHDL	37.8 ± 2.2	24.0 ± 1.5	4.1 ± 0.8	34.1 ± 3.3	83.0 ± 3.3

Mean of duplicate assays from three or more experiments ± SD.

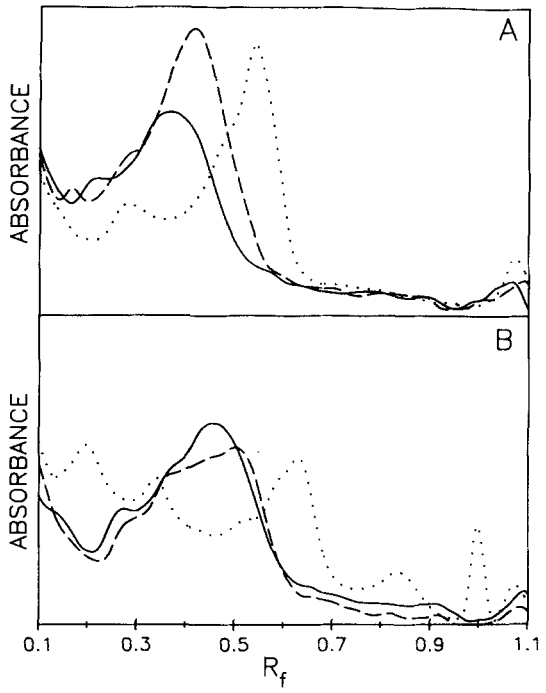

Fig. 6. Densitometric scanning of pore-limit electrophoresis gels of incubated HDL. Incubations of cHDL (panel A) and gHDL (panel B) were conducted for 24 h at 37°C with the addition of d > 1.21 g/ml fraction from control rat sera (-----) or with the addition of d > 1.21 g/ml + d > 1.07 g/ml fractions control rat sera (——). Scans of unincubated HDL are included for comparison (·····). R_f values are for distance migrated for the sample relative to the distance migrated for BSA run on the same gel.

Incubation of gHDL subfractions with purified human LCAT

To determine whether the conversion of gHDL to a form that closely resembled cHDL was as a result of LCAT or other serum components, individual fractions of gHDL were incubated with purified human LCAT. Incubation of apoE-rich gHDL with purified human LCAT and bovine serum albumin at 37°C for 24 h resulted in a general decrease in Stokes diameters of these HDL. Unincubated $gHDL_{30}$ contains two prominent bands of Stokes diameters 31.0 and 28.0 nm, but after incubation the Stokes diameter of the larger band was unchanged and the band at 28 nm was replaced by two bands of 16.0 and 17.1 nm. The Stokes diameters of $gHDL_{16}$ were also decreased after incubation with a disappearance of the 16.7 and 15.2 nm bands and the appearance of a 12.1 nm band. The apoA-I-rich gHDL showed an increase in Stokes diameter following incubation with human LCAT and albumin. With incubation $gHDL_{11}$ showed only a slight increase from 10.6 to 10.8 nm, while $gHDL_8$ showed an increase from 7.7 to 9.0 nm (data not shown).

The cross-linking patterns for the incubated HDL (**Fig. 8**) confirmed the trend observed with the Stokes diameters. The protein mass per particle of apoE-rich gHDL was decreased, while that for the apoA-I rich gHDL increased upon incubation with LCAT + albumin. For all the gHDL subfractions, incubation with LCAT + albumin produced an HDL that showed a prominent band in the region of an apoA-I tetramer after cross-linking. There was also a general decrease in the apoE cross-linked bands, especially the dimer band, with this incubation.

Changes in composition upon incubation of the gHDL subfractions with LCAT + albumin (**Table 5**) were similar to those observed for the incubation of gHDL + d > 1.21 g/ml + d< 1.07 g/ml. There were gains in CE and protein with losses in FC and PL and an increased percentage cholesterol esterification for all the subfractions. However, for the incubated apoE-rich species, $gHDL_{30}$ and $gHDL_{16}$, the percentages of protein and CE were still less and the percentages of FC and PL were still more than for cHDL. While the percentage cholesterol esterification increased five-fold for $gHDL_{30}$ from 8.7 to 46.3% and fourfold for $gHDL_{16}$ from 16.0 to 66.3%, these levels remained lower than that of unincubated cHDL (85.9%).

For $gHDL_{11}$, the level of esterification reached 96.8% with incubation with LCAT, which surpassed the value

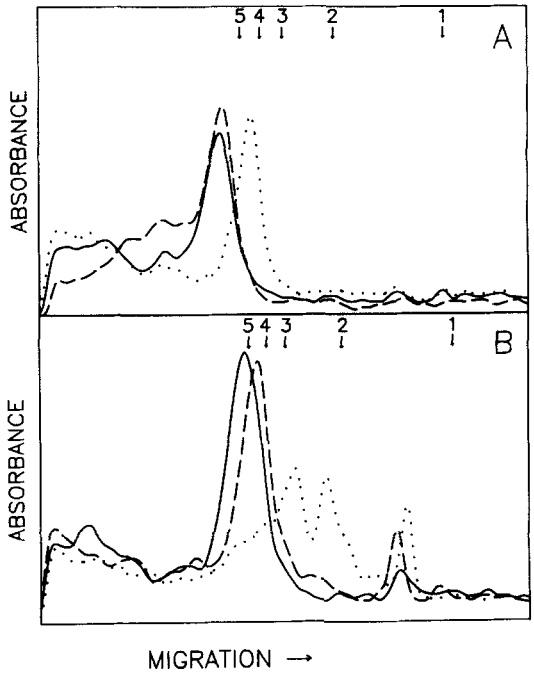

Fig. 7. Densitometric scanning of chemically cross-linked incubated HDL applied to SDS-PAGE gels. Incubations of cHDL (panel A) and gHDL (panel B) were conducted as described in Fig. 6: HDL + d > 1.21 g/ml (-----), HDL + d > 1.21 + d < 1.07 g/ml (——), and unincubated HDL (·····). Positions of the self-associated forms of apoA-I (monomer through pentamer) are indicated by the arrows at the top of the panels.

TABLE 4. Composition of incubated HDL species

Sample	Weight % Composition					% Cholesterol as Ester
	Prot.	PL	FC	CE	TG	
gHDL	33.0	46.0	14.2	6.6	0.2	21.6
gHDL + d>1.21[a]	34.9	34.4	7.7	22.9	nd[c]	63.5
gHDL + d>1.21 + d<1.07[b]	39.3	28.8	5.4	26.7	nd	74.4
cHDL	40.9	26.2	4.4	28.4	0.2	79.2
cHDL + d>1.21[a]	45.2	18.2	0.7	35.9	nd	96.9
cHDL + d>1.21 + d<1.07[b]	45.0	17.6	2.2	35.1	nd	90.3

[a]Incubation was conducted at 37°C for 24 h. HDL concentration was 0.4 mg/ml and the d>1.21 g/ml fraction from control rat serum was added as an LCAT source.
[b]As above with the addition of the d<1.07 g/ml fraction from control rat serum.
[c]Not determined.

for incubated cHDL (92.0%). Even though a level of almost 100% esterification was reached, the composition of this HDL still differed from cHDL in that the weight percentage of CE was lower and the percentage of PL higher than for cHDL. An additional source of free cholesterol appears to be necessary for conversion of this HDL to a form identical to cHDL. The smaller apoA-I-rich gHDL, $gHDL_8$, also appeared to need a source of free cholesterol, as the percentage of CE was lower than for cHDL (10.0 vs. 33.8%) after incubation with LCAT. The percentage of PL had decreased by half for this HDL with incubation, which may result from generalized instability of this HDL or from phospholipolysis in excess of that required for cholesteryl ester formation, as has been

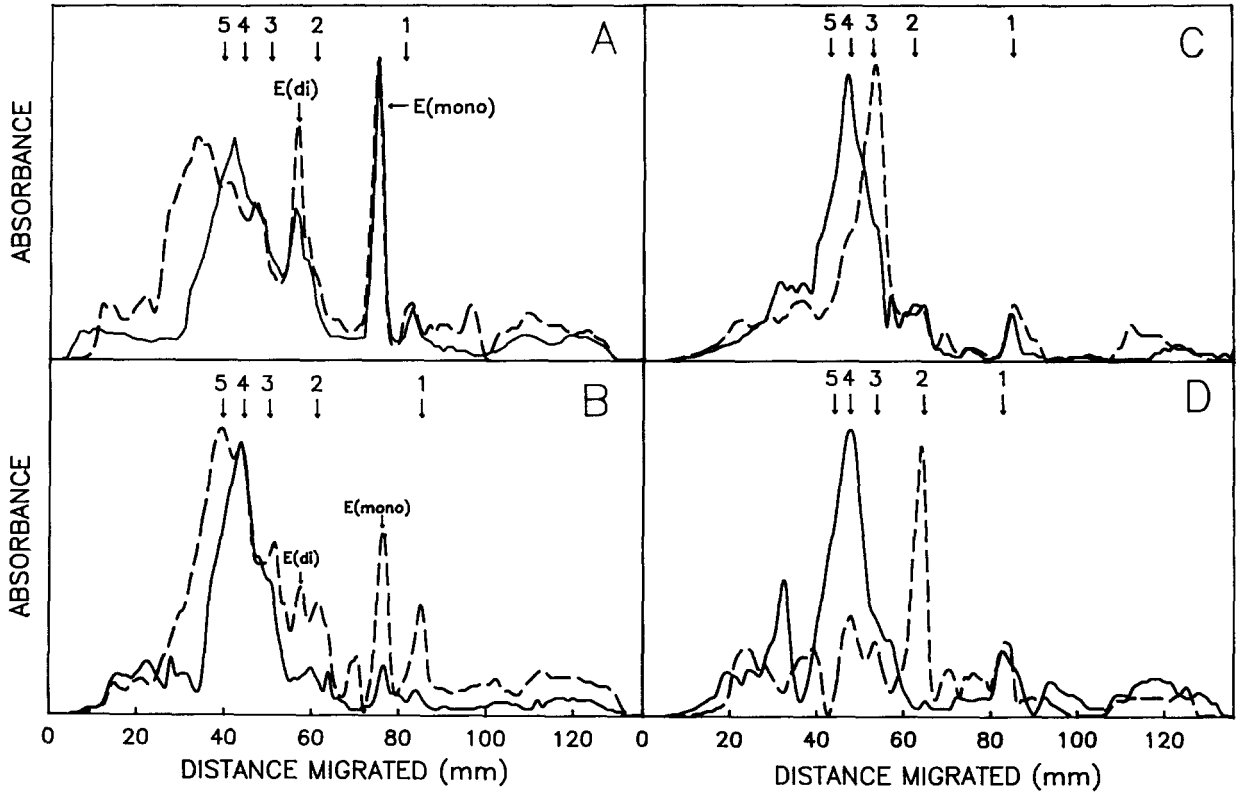

Fig. 8. Densitometric scanning of chemically cross-linked individual gHDL fractions applied to SDS-PAGE gels with (——) or without (-----) LCAT modification. The individual gHDL fractions were modified by incubation for 24 h at 37°C with purified human LCAT (110 U/ml) + BSA (5 g/dl) and reisolated by density ultracentrifugation at d 1.23 g/ml. The apoE rich species, $gHDL_{30}$ (panel A) and $gHDL_{16}$ (panel B), are shown on the left and the apoA-I-rich species, $gHDL_{11}$ (panel C) and $gHDL_8$ (panel D), on the right. The positions of the self-associated forms of apoA-I are indicated by the arrows at the top of the panels. Additionally, apoE monomer (E(mono)) and dimer (E(di)) bands are indicated for the apoE-rich gHDL (panels A and B).

TABLE 5. Composition of HDL species incubated with purified LCAT

HDL	Weight % Composition				% Cholesterol as Ester
	Prot.	PL	FC	CE	
gHDL	25.0	53.4	15.6	6.1	18.7
gHDL + BSA[a]	24.3	43.8	19.5	12.4	26.8
gHDL + LCAT[b]	28.8	43.3	11.2	16.7	46.9
gHDL	16.3	60.6	19.9	3.2	8.7
$gHDL_{30}$ + LCAT[b]	20.6	43.6	14.5	21.3	46.3
$gHDL_{16}$	23.7	55.6	15.7	5.0	16.0
$gHDL_{16}$ + LCAT[b]	26.8	39.5	7.8	25.9	66.3
$gHDL_{11}$	33.7	44.6	5.0	16.7	66.4
$gHDL_{11}$ + LCAT[b]	40.2	31.4	0.5	27.8	96.8
$gHDL_8$	48.8	40.7	3.0	7.5	59.4
$gHDL_8$ + LCAT[b]	66.9	20.2	2.8	10.0	69.1
cHDL	39.5	23.5	3.3	33.8	85.9
cHDL + BSA[a]	43.0	19.3	3.1	34.5	86.9
cHDL + LCAT[b]	49.8	15.0	1.7	33.5	92.0

Assays were conducted in duplicate with the exception of the cholesterol assays for $gHDL_8$ + LCAT, which were single determinants.

[a]Incubation was conducted at 37°C for 24 h. HDL concentration was 0.4 mg/ml, bovine serum albumin concentration was 5 g/dl, and β-mercaptoethanol concentration was 5 mM. HDL was reisolated by density ultracentrifugation at d 1.23 g/ml.

[b]As above with the addition of purified human LCAT (110 U/ml).

observed with LCAT modification of synthetic substrates by Nichols and colleagues (30). The recovery of $gHDL_8$ protein after incubation and density gradient ultracentrifugation was only 25% as compared to 60–75% for the other incubated HDL.

DISCUSSION

Galactosamine treatment was originally proposed as an experimental model for viral hepatitis (31) and was later suggested by Nordby and colleagues (32) to be a useful system for studying the interrelationship between LCAT and lipoprotein secretion. Since that time a great deal more has been learned about the organ contributions to the synthesis of the HDL, but considerable uncertainty exists regarding the pathways whereby the various precursor forms of HDL interact to generate the plasma forms of HDL that have been most widely studied. In this investigation we have utilized the galactosamine-treated rat as a tool to generate, in vivo, HDL species that have been largely unmodified by LCAT in order to understand the effects of cholesterol esterification on these particles.

A number of model systems have been proposed to study newly secreted lipoproteins (3–7, 10). In common with the HDL isolated from the galactosamine-treated rat, these HDL contain a relative abundance of either one or both of the most frequently reported forms of newly secreted HDL: small, apoA-I-rich spherical particles and large, apoE-rich discs.

Similarities in size and composition of the various small HDL are evident (**Table 6**). All are enriched in protein and phospholipid and are in the size range of 7.5–7.8 nm.

TABLE 6. Composition of small apoA-I-rich HDL

HDL	Weight % Composition					% Cholesterol as Ester	Stokes Diameter	Ref.
	Prot.	PL	FC	CE	TG			
$gHDL_8$	51	39	3.5	6.9		54	7.8	
Obstructive jaundice	51	33	5.1	5.6	6.3	39	7.6	7
HepG2 fraction IV	64	31	4.9	0.8		9	7.6	10
LCAT deficiency plasma (MR)[a]	59	35	4.3	0.7	1.4	9	6.0[b]	11
LCAT deficiency plasma (DJ)[a]	60	34	1.3	1.7	2.1	43	6.1[b]	11
Liver perfusate (monkey)	45	46	3.7	3.4	1.8	35	7.8	4
Mesenteric lymph (rat)	61	29	2	7	1	67	7.8	9

[a]Recalculated using the following molecular weights: 28,3000 for A-I, 775 for PL, 386 for FC, 655 for CE, and 850 for TG.

[b]Non-hydrated diameter; correction for hydration increases these values to 7.5–7.6 nm.

This species of HDL is seen to possess only a minor proportion of cholesteryl ester and triglyceride, resulting in a particle with only a small amount of core lipid. It should be noted that, whereas this small HDL is a major species in samples derived from human tissues, it is a relatively minor component in the galactosamine-treated rat.

The apoE-rich gHDL also show many similarities to apoE-rich HDL populations isolated from other sources (**Table 7**) in that they are enriched in phospholipid and free cholesterol and contain little cholesteryl ester (5, 33–35). However, the weight percentage of protein for the gHDL subfractions was the lowest of the apoE-rich HDL. This may, in part, be attributed to the generalized inhibitory action of galactosamine on UDP-dependent processes such as protein synthesis, although, in general, the rat HDL possess a lower percentage of protein than human HDL.

Thus, galactosamine treatment in the rat generates a heterogeneous population of HDL species with chemical and physical properties closely resembling other models of nascent HDL. We find that the subpopulations that we have isolated are useful analogs to nascent HDL species despite the fact that the induced hepatotoxicity can cause a number of metabolic aberrations. For example, although LCAT deficiency is a major consequence of this treatment Black, Freeman, and Sabesin (36) have reported that both hepatic and lipoprotein lipase are inhibited in the galactosamine-treated rat to 23.2% and 37.6% of control values, respectively. Presumably, the HDL would therefore be subject to even less post-secretory modification than control HDL.

We note that 24 h after treatment there was essentially no HDL remaining that could be identified as equivalent to control HDL. The $t_{1/2}$ for rat HDL_2, the major HDL species in rat plasma, was shown to be 10 h when the protein was radiolabeled (37), but 6–7 h when the cholesteryl ester was radiolabeled (38). As serum from galactosamine-treated rats is collected 24 h after treatment, this would correspond to either two or four half-lives with 25% or 6.25% of the starting HDL_2 pool remaining, respectively. The lack of HDL of the size of cHDL in the gHDL fraction would suggest that the $t_{1/2}$ of 6–7 h may be more applicable to this model and that little or no cHDL-type particles are generated after treatment. Additionally, HDL_2 can be converted to the larger HDL_1, but as this process appears to be LCAT-mediated (39), its contribution to the disappearance of HDL_2 in the galactosamine-treated rat may be minor.

Control HDL and gHDL also differed in their surface properties, as evidenced by marked differences in protein cross-linking patterns. While the cHDL formed essentially a single broad band corresponding to a protein mass of 153,000, multiple bands were seen for cross-linked gHDL, most of which were smaller than what might have been expected based upon migration by pore-limit electrophoresis. The individual apoA-I-rich gHDL subfractions did generate defined cross-linked bands corresponding to the expected protein mass per particle and suggested the presence of two apoA-I per particle for $gHDL_8$, and three apoA-I per particle for $gHDL_{11}$. All the apoE-rich gHDL subfractions, however, cross-linked poorly and apoE monomer, dimer, and sometimes trimer bands were prominent. It is not known whether this inability to cross-link the proteins of these particles is a property of apoE or whether the free amino groups of the proteins are too widely spaced for or somehow inaccessible to the cross-linker. Rat apoE has been found to contain considerably less lysine than rat apoA-I (11 lysines per molecule for apoE vs. 21 lysines per molecule for apoA-I (27, 40), so that substituting apoE for apoA-I could possibly lead to decreased cross-linking of HDL protein, although apoE present in control HDL appears to cross-link normally (Fig. 5, lane 9, and ref. 29). It does appear that an increased content of apoE is associated with a decreased ability of the proteins of gHDL particles to be cross-linked. However, a correlation between an in-

TABLE 7. Composition of large apoE-rich HDL

HDL	Weight % Composition					% Cholesterol as Ester	Stokes Diameter	Ref.
	Prot.	PL	FC	CE	TG			
$gHDL_{35+}$	22	50	25	3.1		6.6	35[a]	
$gHDL_{30}$	14	59	23	3.7		8.5	30[a]	
$gHDL_{16}$	23	55	18	5.0		14.3	16[a]	
HepG2 fraction I	25	51	23	1.3		3.2	22[b]	10
HepG2 fraction II	28	47	23	1.5		3.8	19[b]	10
LCAT deficiency plasma (MR)[c]	30	50	19				20[b]	5
LCAT deficiency plasma (AA)[c]	29	47	24				28[b]	5
Rat liver perfusate + DTNB	38	40	12	4.3	5.4	17.3	19[b]	33

[a]Diameters measured by gradient gel electrophoresis.
[b]Diameters measured by electron microscopy.
[c]Recalculated using the following molecular weights: 28,300 for A-I, 775 for PL, 386 for FC, 655 for CE, and 850 for TG.

creasing content of apoE with increasing particle diameter is also evident, so that decreased cross-linking could be simply attributed to greater distances between reactive groups as might be expected for these large protein-poor HDL. Attempts to cross-link the proteins of such large particles as VLDL have failed to demonstrate effective intermolecular cross-links (M. W. Orishimo and J. B. Swaney, unpublished data). Additionally, it has been shown that the apoE-rich gHDL are discoidal particles (12) as compared to spherical cHDL, but it is not known how such a morphology may influence the availability of free amino groups to the cross-linking reagent.

Nascent HDL are often defined by their ability to be transformed into mature plasma HDL by the action of LCAT. The suitability of apoE-rich HDL as compared to apoA-I-rich HDL as LCAT substrates has been disputed. Utermann et al. (41) incubated serum from LCAT-deficient patients with purified LCAT and found that the apoE-rich HDL were not transformed into plasma-like HDL as the other HDL species were. Marcel et al. (2) found that apoE-rich HDL from LCAT-deficient patients did serve as LCAT substrates and were in fact better substrates than normal plasma apoA-I-rich HDL. However, the apoA-I HDL from these patients were still better substrates than their apoE-rich HDL.

In agreement with the findings of Marcel et al. (2) both the apoA-I- and apoE-rich gHDL were found to be suitable substrates for LCAT. It was seen that, although neither type of gHDL was converted to a form identical to control plasma HDL when they were incubated with purified human LCAT alone, higher levels of cholesteryl esterification were achieved for the apoA-I-rich gHDL than for the apoE-rich gHDL. However, a much greater increase in percent esterification was achieved for the apoE-rich gHDL, even though the ratio of LCAT activity units/nmol substrate cholesterol was much less for these cholesterol-rich HDL (Table 5).

One question of particular interest was whether the various types of HDL seen in galactosamine treatment or with other models of nascent HDL are merged in some manner to yield mature HDL. It was found that incubation of gHDL with the lipoprotein-free $d > 1.21$ + the $d < 1.07$ g/ml density fractions from control rat serum resulted in the formation of an HDL species that by size and composition was essentially identical to unincubated control HDL. The many different species normally seen with gradient gel electrophoresis of gHDL were replaced with a single broad band (Fig. 6). It was also found that incubation of gHDL with the lipoprotein-free fraction alone led to the disappearance of the heterogeneous gHDL pattern, yielding a broad banded species, but the composition differed from control HDL in that the protein and cholesteryl ester content was still lower and the free cholesterol and phospholipid content was still higher. It is also important to note that by cross-linking (Fig. 7) the heterogeneous pattern was replaced by a pattern rather similar to control HDL. This suggests that the particles might undergo a fusion, similar to that described with synthetic HDL species (42) and physiological HDL (11), resulting in a mature form containing multiple types of apolipoproteins. This is of particular significance for apoE, since it may modulate receptor-mediated uptake of particles.

It is uncertain whether all the gHDL are synthesized as nascent particles or whether some of them are conversion products. In particular, $gHDL_{11}$ may be produced from $gHDL_8$ within the plasma compartment as a result of gains of phospholipid and cholesterol and of LCAT activity on the particle. A 24-h incubation of $gHDL_8$ with purified human LCAT did produce an HDL population that included HDL with three apoA-I per particle, but there was not sufficient sample available to determine the composition of these HDL (J. E. Matsuura and J. B. Swaney, unpublished data).

In summary, we have found that the galactosamine-treated rat, which was shown by others to be an interesting model for LCAT deficiency, generates a wide variety of particles that appear to have very similar properties to other species of nascent HDL that have been studied. These gHDL subfractions all serve as LCAT substrates and despite their quite varied compositions are transformed into a form essentially identical to plasma HDL when gHDL is incubated with the lipoprotein-free fraction + the $d < 1.07$ g/ml fractions from control rat serum. Thus, a condensation seems to occur that reduces the heterogeneity of the sample and alters the surface properties of these species. These HDL are, we believe, useful for study as newly secreted lipoprotein particles contained within the plasma compartment that have undergone minimal LCAT modification.

The authors would like to acknowledge the contributions and excellent technical assistance which were provided in this project by Ms. Margaret Orishimo. Helpful advice on purification of the LCAT enzyme was gratefully received from Dr. Ana Jonas and Mr. Frank Bonelli. This research was supported by Research Grant HL-33827 from the National Institutes of Health.
Manuscript received 13 August 1990 and in revised form 26 December 1990.

REFERENCES

1. Ragland, J. B., P. D. Bertram, and S. M. Sabesin. 1978. Identification of nascent high density lipoproteins containing arginine-rich protein in human plasma. *Biochem. Biophys. Res. Commun.* **80:** 81–88.
2. Marcel, Y. L., C. Vezina, D. Emond, and G. Suzue. 1980. Heterogeneity of human high density lipoprotein: presence of lipoproteins with and without apoE and their roles as substrates for lecithin:cholesterol acyltransferase reaction. *Proc. Natl. Acad. Sci. USA.* **77:** 2969–2973.
3. Hamilton, R. L., M. C. Williams, C. J. Fielding, and R. J. Havel. 1976. Discoidal bilayer structure of nascent

high density lipoproteins from perfused rat liver. *J. Clin. Invest.* **58:** 667–680.
4. Babiak, J., H. Tamachi, F. L. Johnson, J. S. Parks, and L. L. Rudel. 1986. Lecithin:cholesterol acyltransferase-induced modifications of liver perfusate discoidal high density lipoproteins from African green monkeys. *J. Lipid Res.* **27:** 1304–1317.
5. Mitchell, C. D., W. C. King, K. R. Applegate, T. Forte, J. A. Glomset, K. R. Norum, and E. Gjone. 1980. Characterization of apolipoprotein E-rich high density lipoproteins in familial lecithin:cholesterol acyltransferase deficiency. *J. Lipid Res.* **21:** 625–634.
6. Green, P. H. R., A. R. Tall, and R. M. Glickman. 1978. Rat intestine secretes discoid high density lipoprotein. *J. Clin. Invest.* **61:** 528–534.
7. Clifton, P. M., P. J. Barter, and A. M. Mackinnon. 1988. High density lipoprotein particle size distribution in subjects with obstructive jaundice. *J. Lipid Res.* **29:** 121–135.
8. Hoffman, J. S., and E. P. Benditt. 1982. Secretion of serum amyloid protein and assembly of serum amyloid protein-rich high density lipoprotein in primary mouse hepatocyte culture. *J. Biol. Chem.* **257:** 10518–10528.
9. Forester, G. P., A. R. Tall, C. L. Bisgaier, and R. M. Glickman. 1983. Rat intestine secretes spherical high density lipoproteins. *J. Biol. Chem.* **258:** 5938–5943.
10. McCall, M. R., T. M. Forte, and V. G. Shore. 1988. Heterogeneity of nascent high density lipoproteins secreted by the hepatoma-derived cell line, Hep G2. *J. Lipid Res.* **29:** 1127–1137.
11. Chen, C., K. Applegate, W. C. King, J. A. Glomset, K. R. Norum, and E. Gjone. 1984. A study of the small spherical high density lipoproteins of patients afflicted with familial lecithin:cholesterol acyltransferase deficiency. *J. Lipid Res.* **25:** 269–282.
12. Sabesin, S. M., L. B. Kuiken, and J. B. Ragland. 1975. Lipoprotein and lecithin:cholesterol acyltransferase changes in galactosamine-induced rat liver injury. *Science.* **190:** 1302–1304.
13. Decker, K., and D. Keppler. 1972. Galactosamine-induced liver injury. *Prog. Liver Dis.* **4:** 183–199.
14. Cartwright, C. K., J. B. Ragland, S. W. Weidman, and S. M. Sabesin. 1982. Alterations in lipoprotein composition associated with galactosamine-induced rat liver injury. *J. Lipid Res.* **23:** 667–679.
15. Ji, T. H. 1973. Interference by detergents, chelating agents, and buffers with the Lowry protein determination. *Anal. Biochem.* **52:** 517–521.
16. Blanche, P. J., E. L. Gong, T. M. Forte, and A. V. Nichols. 1981. Characterization of human high density lipoproteins by gradient gel electrophoresis. *Biochim. Biophys. Acta.* **665:** 408–419.
17. Gidez, L. I., J. B. Swaney, and S. Murnane. 1977. Analysis of rat serum apolipoproteins by isoelectric focusing. I. Studies on the middle molecular weight subunits. *J. Lipid Res.* **18:** 59–68.
18. Swaney, J. B., and K. O'Brien. 1978. Cross-linking studies of the self-association properties of apo-A-I and apo-A-II from human high density lipoprotein. *J. Biol. Chem.* **253:** 7069–7077.
19. Markwell, M. A., S. M. Haas, L. L. Bieber, and N. E. Tolbert. 1978. A modification of the Lowry procedure to simplify protein determination in membrane and lipoprotein samples. *Anal. Biochem.* **87:** 206–210.
20. Sokoloff, L., and G. H. Rothblat. 1974. Sterol to phospholipid molar ratios of L cells with qualitative and quantitative variations of cellular sterol. *Proc. Soc. Exp. Biol. Med.* **146:** 1166–1172.
21. Matz, C. E., and A. Jonas. 1982. Reaction of human lecithin:cholesterol acyltransferase with synthetic micellar complexes of apolipoprotein A-I, phosphatidylcholine, and cholesterol. *J. Biol. Chem.* **257:** 4541–4546.
22. Bradford, M. 1976. A rapid and sensitive method for the quantitation of microgram quantities of protein utilizing the principle of protein-dye binding. *Anal. Biochem.* **72:** 248–255.
23. Chen, C. H., and J. J. Albers. 1983. Interspecies activation of lecithin-cholesterol acyltransferase by apolipoprotein A-I isolated from the plasma of humans, horses, sheep, goats and rabbits. *Biochim. Biophys. Acta.* **753:** 40–46.
24. Swaney, J. B. 1980. Mechanisms of protein-lipid interaction. Association of apolipoproteins A-I and A-II with binary phospholipid mixtures. *J. Biol. Chem.* **255:** 8791–8797.
25. Lasser, N. L., P. S. Roheim, D. Edelstein, and H. A. Eder. 1973. Serum lipoproteins of normal and cholesterol-fed rats. *J. Lipid Res.* **14:** 1–8.
26. Boguski, M. S., N. Elshourbagy, J. M. Taylor, and J. I. Gordon. 1984. Rat apolipoprotein A-IV contains 13 tandem repetitions of a 22-amino acid segment with amphipathic helical potential. *Proc. Natl. Acad. Sci. USA.* **81:** 5021–5025.
27. Swaney, J. B., F. Braithwaite, and H. A. Eder. 1977. Characterization of the apolipoproteins of rat plasma lipoproteins. *Biochemistry.* **16:** 271–278.
28. Dory, L., L. M. Boquet, R. L. Hamilton, C. H. Sloop, and P. S. Roheim. 1985. Heterogeneity of dog interstitial fluid (peripheral lymph) high density lipoproteins: implications for a role in reverse cholesterol transport. *J. Lipid Res.* **26:** 519–527.
29. Swaney, J. B., M. W. Orishimo, and A. Girard. 1987. Enzymatically induced alterations in the structure of rat serum lipoproteins. *J. Lipid Res.* **28:** 982–992.
30. Nichols, A. V., P. J. Blanche, E. L. Gong, V. G. Shore, and T. M. Forte. 1985. Molecular pathways in the transformation of model discoidal lipoprotein complexes induced by lecithin:cholesterol acyltransferase. *Biochim. Biophys. Acta.* **834:** 285–300.
31. Keppler, D., R. Lesch, W. Reutter, and K. Decker. 1968. Experimental hepatitis induced by D-galactosamine. *Exp. Molec. Pathol.* **9:** 279–290.
32. Nordby, G., B. Schreiner, T. Berg, and K. R. Norum. 1977. The effect of D-galactosamine on LCAT secretion and ultrastructure of isolated rat hepatocytes. *Acta. Pathol. Microbiol. Scand. [A].* **85:** 839–849.
33. Hamilton, R. L., L. S. S. Guo, T. E. Felker, Y-S. Chao, and R. J. Havel. 1986. Nascent high density lipoproteins from liver perfusates of orotic acid-fed rats. *J. Lipid Res.* **27:** 967–978.
34. Roheim, P. S., D. Rachmilewitz, O. Stein, and Y. Stein. 1971. Metabolism of iodinated high density lipoproteins in the rat. 1. Half-life in the circulation and uptake by organs. *Biochim. Biophys. Acta.* **248:** 315–329.
35. Dallinga-Thie, G. M., P. H. Groot, and A. van Tol. 1985. Distribution of apolipoprotein A-IV among lipoprotein subclasses in rat serum. *J. Lipid Res.* **26:** 970–976.
36. Black, D. D., M. R. Freeman, and S. M. Sabesin. 1982. Lipoprotein lipase and hepatic lipase deficiencies associated with impaired chylomicron clearance in D-(+)-galactosamine hepatitis. *Metabolism.* **31:** 620–626.
37. Roheim, P. S., H. Hirsch, D. Edelstein, and D. Rashmile-

witz. 1972. Metabolism of iodinated high density lipoprotein subunits in the rat. III. Comparison of the removal of different subunits from the circulation. *Biochim. Biophys. Acta.* **278:** 517–529.
38. Eisenberg, S., Y. Oschry, and J. Zimmerman. 1984. Intravascular metabolism of the cholesteryl ester moiety of rat plasma lipoproteins. *J. Lipid Res.* **25:** 121–128.
39. Eisenberg, S. 1984. High density lipoprotein metabolism. *J. Lipid Res.* **25:** 1017–1058.
40. McLean, J W., C. Fukazawa, and J. M. Taylor. 1983. Rat apolipoprotein E mRNA: cloning and sequencing of double-stranded cDNA. *J. Biol. Chem.* **258:** 8993–9000.
41. Utermann, G., H-J. Menzel, G. Adler, P. Dieker, and W. Weber. 1980. Substitution in vitro of lecithin cholesterol acyltransferase: analysis of changes in plasma lipoproteins. *Eur. J. Biochem.* **107:** 225–241.
42. Nichol, A. V. 1990. Conversions in the origins and metabolism of human plasma HDL. *In* Advances in Cholesterol Research. M. Esfahani and J. B. Swaney, editors. Telford Press, Caldwell, NJ. 315–365.